IJE TRANSACTIONS C: Aspects Vol. 26, No. 6, (June 2013) 641-652

International Journal of Engineering

Journal Homepage: www.ije.ir

A General Solution for Implicit Time Stepping Scheme in Rate-dependant Plasticity

F. Moayyedian *, M. Kadkhodayan

Department of Mechanical Engineering, Ferdowsi University of Mashhad, 91775-1111, Mashhad, Iran

PAPER INFO

Paper history:
Received 23 October 2012
Received in revised form 01 December 2012
Accepted 13 December 2012

Keywords:
Rate-dependant Plasticity
Time Stepping Schemes
Implicit
Thick Walled Cylinder

ABSTRACT

In this paper derivation of the second differentiation of a general yield surface by implicit time stepping method along with its consistent elastic-plastic modulus is studied. Moreover, the explicit, trapezoidal implicit and fully implicit time stepping schemes are compared in rate-dependant plasticity. It is shown that implementing fully implicit time stepping scheme in rate-dependant plasticity predicts more accurate experimental results than other schemes.

doi: *10.5829/idosi.ije.2013.26.06c.09*

1. INTRODUCTION

Viscoplasticity describes the rate-dependent inelastic behavior of solids. Rate-dependence in this context means that the deformation of the material depends on the rate at which loads are applied. The inelastic behavior of viscoplasticity is a plastic deformation and means that the material undergoes unrecoverable deformations when a certain load level is reached. Rate-dependent plasticity is usually an important task because of its transient plasticity calculations. The main difference between the rate-independent plastic and viscoplastic material models is that the latter exhibits not only permanent deformations, but continues to undergo a creep flow as a function of time under the applied load. Some studies of the previous researchers on the mentioned subject are reviewed here.

Krieg and Krieg [1] investigated the accuracy of the integration of the constitutive equations for an isotropic elastic-perfectly plastic von Mises material. Simo and Taylor [2] demonstrated the concept of consistency between the tangent operator and the integration algorithm. Dodds [3] derived an extension of elastic-plastic-radial return algorithm and a consistent tangent operator which satisfy the requirements for stable, accurate and efficient numerical procedure for plane stress condition with mixed hardening. Gratacos et al. [4] investigated the generalized midpoint rule for the time integration of elastic-plastic constitutive equations for pressure-independent yield criteria. Kadkhodayan and Zhang [5] proposed a new efficient method, the consistent DXDR method, to analyze general elastic-plastic problems. In recent years, Kang [6] proposed a visco-plastic constitutive model to simulate the uniaxial/multiaxial ratcheting of cyclically stable materials. Kumar and Nukala [7] presented a return mapping algorithm for cyclic viscoplastic constitutive models. Ding et al. [8] developed a stress integration scheme to analyze a three-dimensional sheet metal forming problems. Liang et al. [9] presented a design sensitivity analysis method including geometry, elasto-visco-plastic material and boundary conditions parameters. Khosroshahi and Sadrnejad [10] proposed a framework including damage progress for simulating behavior of concrete under multiaxial loading for the constitutive model based on the semi-micromechanical aspects of plasticity. Romano and Diaco [11] introduced a consistent tangent stiffness to improve the asymptotic convergence rate of the iterative correction algorithm for analysis of elastoplastic structures. Rezaiee-Pajand and Sinaie [12] investigated the strain space formulation. Numerical examples were analyzed using the traditional linear method and their suggested schemes using von Mises yield criterion and Prager's linear hardening rule. Karrech et al. [13] introduced a comprehensive model that was capable to describe the behavior under cyclic loading. Voyiadjis et al. [14] developed a thermodynamic consistent, small-strain,

*Corresponding Author Email: *farzad_moayyedian@yahoo.com* (F. Moayyedian)

non-unified model to capture the irregular rate dependency including strain controlled inelastic responses of polymers at the glassy state. Graham et al. [15] presented a specimen that can be tested in combined tension and torsion to achieve low triaxiality over a range of Lode angle. Two important factors in time stepping schemes are accuracy and stability. In explicit time stepping schemes the time interval plays a crucial role in stability and accuracy, i.e. a very large time interval cannot guarantee the stability and accuracy of the algorithm. On the other hand, in implicit time stepping schemes, even by choosing a large time interval, the stability is guaranteed. In fact, this is the main advantage of implicit to explicit time stepping algorithms. However, choosing a large time interval may not give proper accuracy.

The main aim of the present study is to obtain a simplified matrix formulation of a general yield criterion for an implicit time stepping scheme in a global finite element method and comparing three time stepping scheming methods in rate-dependent plasticity. The current proposed method is obtained based on the development of techniques given in references [16-20] and [21-25] in FE and plasticity theories, respectively. To show the capability of the method, it is implemented for an internally elastic-viscoplastic pressurized thick walled cylinder with perfectly plastic and linear-isotropic hardening behavior. The provided program is coded in Compaq Visual Fortran Professional Edition 6.5.0.

There are two novel points in the current study for viscoplastic materials.. First, the analytical derivation of the first and the second differentiation of a general criterion, and second, the comparison between the time stepping schemes for different criteria and also using perfect and linear hardening behaviors of materials. Figure 1 shows the flowchart of the program for two-dimensional elastic-viscoplastic applications for a global finite element program [16].

2. GENERAL FORM OF A YIELDING CRITERION

The general form of a yield surface for isotropic materials is $F(J_1,J_2',J_3')$, where J_1 is the first invariant of stress and J_2' and J_3' are the second and the third invariants of deviatoric stresses, respectively. Whereas J_1 indicates the dependence of the yield surface to the hydrostatic pressure and J_2' and J_3' show the dependence of the yield surface to deviatoric stresses. Introducing θ as the angle of loading in deviatoric plane we have [16]:

$$\sin 3\theta = -\frac{3\sqrt{3}}{2}\frac{J_3'}{(J_2')^{\frac{3}{2}}} \quad (1)$$

The angle of θ represents the direction of the loading vector in the deviatoric plane, see Figure 2. For an isotropic material it would be sufficient if the yield surface is studied only in the region of $-\frac{\pi}{6} \le \theta \le +\frac{\pi}{6}$. Hence, because the Lode parameter is defined as $\Gamma = -\sqrt{3}\tan\theta$, the yield surfaces can be studied in $-1 \le \Gamma \le +1$. Then, for the pure shear we have $\Gamma = \theta = 0$, for pure tension $\theta = -\frac{\pi}{6}$ and $\Gamma = +1$ and for pure compression $\theta = +\frac{\pi}{6}$ and $\Gamma = -1$. The four well-known yield surfaces can be shown in the following form for the computational convenience, where σ_Y is the uniaxial yield stress, κ is the hardening parameter, Φ is the angle of internal friction and c is the cohesion [16], Table 1. Drucker-Prager yield surface has a form of circular cone. In order to make the Drucker-Prager circle coincide with the outer apices of the Mohr-Coulomb hexagon at any section, it can be shown that:

$$\alpha = \frac{2\sin\Phi}{\sqrt{3}(3-\sin\Phi)}, \qquad k' = \frac{6c\cos\Phi}{\sqrt{3}(3-\sin\Phi)}, \quad (2)$$

where the parameters α and k' were employed in Drucker-Prager criterion as it shown in Table 1. In Figure 2 the presentation of the four criteria can be observed in deviatoric plane.

3. CALCULATION OF THE FIRST AND SECOND DIFFERENTIATION OF A YIELDING CRITERION

To employ the implicit time stepping scheme along with the consistent elastic-plastic modulus in global finite element method, we need to compute the first and the second differentiation of the yield surface, $\frac{\partial \vec{F}}{\partial \sigma}$ and $\frac{\partial^2 \vec{F}}{\partial \sigma^2}$ as below. The symbols $\rightarrow$ and $\leftrightarrow$ are used for 6×1 vector and 6×6 matrix in three dimensional stress space, respectively.

3. 1. Calculation of the First Differentiation From Equation (1) it can be shown that:

$$\sin 3\theta = \Phi(J_2', J_3'), \quad (3)$$

therefore, any yield criterion can take the following form:

$$F = F(J_1, J_2', \theta). \quad (4)$$

TABLE 1. Four famous yield criteria [16].

Tresca	$2(J_2')^{\frac{1}{2}}\cos\theta = \sigma_Y(\kappa)$,
von Mises	$\sqrt{3}(J_2')^{\frac{1}{2}} = \sigma_Y(\kappa)$,
Mohr-Coulomb	$\frac{1}{3}J_1\sin\Phi + (J_2')^{\frac{1}{2}}\left(\cos\theta - \frac{1}{\sqrt{3}}\sin\theta\sin\Phi\right) = c\cos\Phi$,
Drucker-Prager	$\alpha J_1 + (J_2')^{\frac{1}{2}} = k'$.

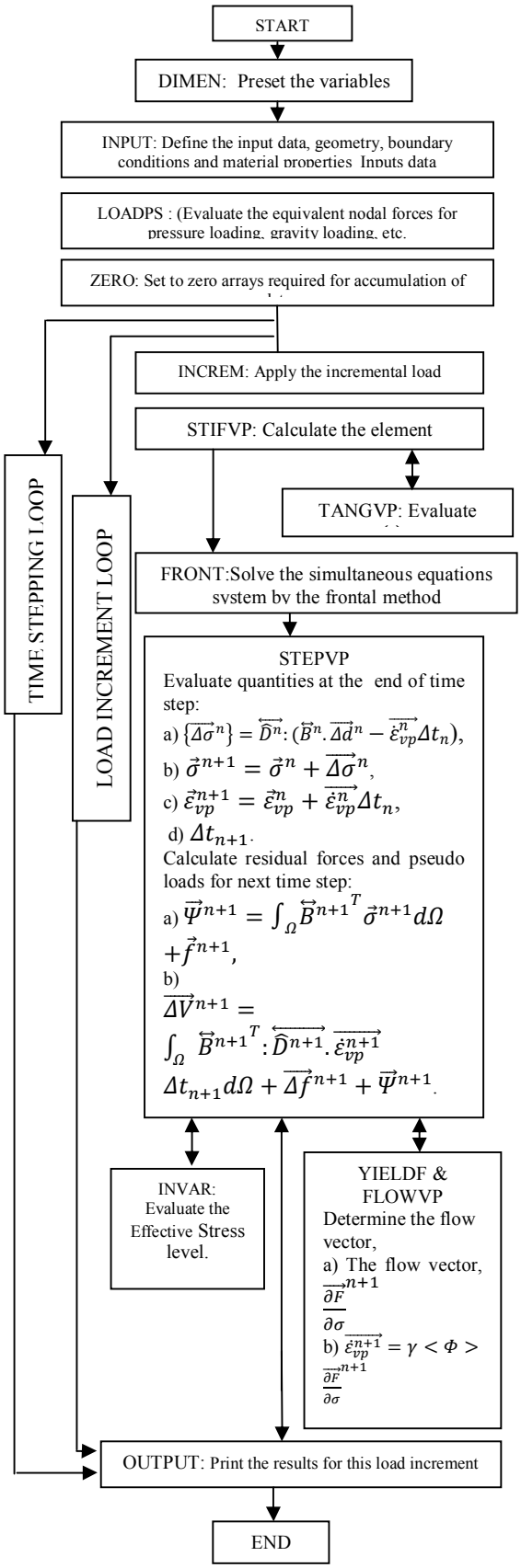

Figure 1. Flow sequence for the two-dimensional elasto-viscoplastic stress analysis program [16]

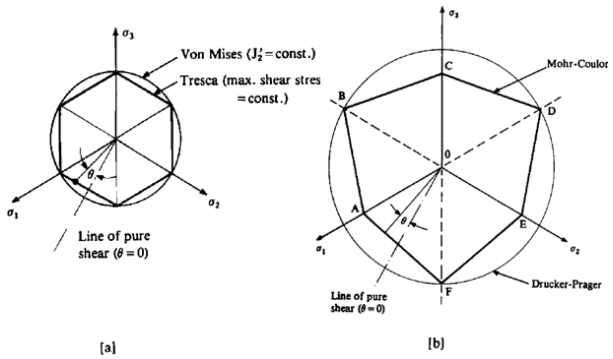

Figure 2. Presentation of four yield surfaces in π plane [16], (a) von Mises and Tresca surfaces, (b) Drucker-Prager and Mohr-Coulomb surfaces.

By differentiating Equation (4):

$$\overrightarrow{\frac{\partial F}{\partial\sigma}} = \frac{\partial F}{\partial J_1}\overrightarrow{\frac{\partial J_1}{\partial\sigma}} + \frac{\partial F}{\partial J_2'}\overrightarrow{\frac{\partial J_2'}{\partial\sigma}} + \frac{\partial F}{\partial\theta}\overrightarrow{\frac{\partial\theta}{\partial\sigma}}. \quad (5)$$

Differentiating Equation (1) gives:

$$\overrightarrow{\frac{\partial\theta}{\partial\sigma}} = \frac{-\sqrt{3}}{2\cos 3\theta}\left(\frac{1}{(J_2')^{\frac{3}{2}}}\overrightarrow{\frac{\partial J_3'}{\partial\sigma}} - \frac{3J_3'}{2(J_2')^{\frac{5}{2}}}\overrightarrow{\frac{\partial J_2'}{\partial\sigma}}\right). \quad (6)$$

Inserting Equation (6) into Equation (5) and with the aid of Equation (1) and after some simplification, it is found that:

$$\overrightarrow{\frac{\partial F}{\partial\sigma}} = C_1\overrightarrow{\frac{\partial J_1}{\partial\sigma}} + C_2\overrightarrow{\frac{\partial J_2'}{\partial\sigma}} + C_3\overrightarrow{\frac{\partial J_3'}{\partial\sigma}}, \quad (7)$$

where values of C_1, C_2 and C_3 and vectors of $\overrightarrow{\frac{\partial J_1}{\partial\sigma}}$, $\overrightarrow{\frac{\partial J_2}{\partial\sigma}}$ and $\overrightarrow{\frac{\partial J_3}{\partial\sigma}}$ are tabulated in Appendix I.

3. 2. Calculation of the Second Differentiation

Considering $\overrightarrow{\frac{\partial F}{\partial\sigma}} = \vec{a}(J_1,J_2,J_3,\vec{\sigma})$, it is found that:

$$\overrightarrow{\frac{\partial^2 F}{\partial\sigma^2}} = \overrightarrow{\frac{\partial a}{\partial J_1}}\otimes\overrightarrow{\frac{\partial J_1}{\partial\sigma}} + \overrightarrow{\frac{\partial a}{\partial J_2'}}\otimes\overrightarrow{\frac{\partial J_2'}{\partial\sigma}} + \overrightarrow{\frac{\partial a}{\partial\theta}}\otimes\overrightarrow{\frac{\partial\theta}{\partial\sigma}} + \overrightarrow{\frac{\partial a}{\partial\sigma}}. \quad (8)$$

Inserting Equation (6) in Equation (8) and with the aid of Equation (1) we have:

$$\overrightarrow{\frac{\partial^2 F}{\partial\sigma^2}} = \overrightarrow{C_1}\otimes\overrightarrow{\frac{\partial J_1}{\partial\sigma}} + \overrightarrow{C_2}\otimes\overrightarrow{\frac{\partial J_2'}{\partial\sigma}} + \overrightarrow{C_3}\otimes\overrightarrow{\frac{\partial J_3'}{\partial\sigma}} + \overrightarrow{\frac{\partial a}{\partial\sigma}} \quad (9)$$

Now, the last term in the right-hand side of Equation (9) can be found by the aid of Equation (7) as following:

$$\overrightarrow{\frac{\partial a}{\partial \sigma}} = C_1 \overrightarrow{\frac{\partial^2 J_1}{\partial \sigma^2}} + C_2 \overrightarrow{\frac{\partial^2 J_2'}{\partial \sigma^2}} + C_3 \overrightarrow{\frac{\partial^2 J_3}{\partial \sigma^2}}, \tag{10}$$

where vectors $\overrightarrow{C_1'}$, $\overrightarrow{C_2'}$ and $\overrightarrow{C_3'}$ and also matrices $\overrightarrow{\frac{\partial^2 J_1}{\partial \sigma^2}}$, $\overrightarrow{\frac{\partial^2 J_2'}{\partial \sigma^2}}$ and $\overrightarrow{\frac{\partial^2 J_3}{\partial \sigma^2}}$ are presented in Appendix II. After some simplifications, the general form of the second differentiation of any yield surface as $F(J_1, J_2', J_3')$ takes the following form:

$$\begin{aligned}\overrightarrow{\frac{\partial^2 F}{\partial \sigma^2}} = & \left(\frac{\partial C_2}{\partial J_2'} - \frac{\tan 3\theta}{2J_2'}\frac{\partial C_2}{\partial \theta}\right)\vec{e} \otimes \\ & \vec{e} + \left(\frac{\partial C_3}{\partial J_2'} - \frac{\tan 3\theta}{2J_2'}\frac{\partial C_3}{\partial \theta}\right)\vec{f} \otimes \vec{e} + C_3 \vec{g} \otimes \vec{e} - \\ & \frac{\sqrt{3}}{2\cos 3\theta}\frac{1}{(J_2')^{\frac{3}{2}}}\frac{\partial C_2}{\partial \theta}\vec{e} \otimes \vec{f} - \frac{\sqrt{3}}{2\cos 3\theta}\frac{1}{(J_2')^{\frac{3}{2}}}\frac{\partial C_3}{\partial \theta}\vec{g} \otimes \\ & \vec{g} + \frac{1}{3}C_2\vec{\vec{M}} + \frac{2}{3}C_3\vec{\vec{N}},\end{aligned} \tag{11}$$

where vectors $\vec{e}$, $\vec{f}$ and $\vec{g}$ along with matrices $\vec{\vec{M}}$ and $\vec{\vec{N}}$ are presented in Appendix III.

4. VISCOPLASTIC FLOW RULE

A common explicit form of an associated viscoplastic strain rate is offered by the following viscoplastic flow rule:

$$\overrightarrow{\dot{\varepsilon}_{vp}} = \gamma < \Phi(F) > \overrightarrow{\frac{\partial F}{\partial \sigma}}, \tag{12}$$

where $F = F(\sigma, \varepsilon_{vp}, \kappa)$ is a yield surface and γ is a fluidity parameter controlling the plastic flow rate. The term $\Phi(F)$ is a positive monotonic increasing function for $x > 0$ and the notation $\langle \quad \rangle$ implies that:

$$\begin{cases} < \Phi(x) > = \Phi(x) & x > 0 \\ < \Phi(x) > = 0 & x \le 0 \end{cases} \tag{13}$$

Different functions for Φ have also been recommended as follows [16]:

$$\begin{cases} \Phi(F) = e^{M\left(\frac{F-F_0}{F_0}\right)} - 1, \\ \Phi(F) = \left(\frac{F-F_0}{F_0}\right)^N, \end{cases} \tag{14}$$

where M and N are arbitrary prescribed constants.

4. 1. The Viscoplastic Strain Increment With the strain rate law expressed by Equation (12) we can define a strain increment $\Delta\varepsilon_{vp}^n$ occurring in a time interval $\Delta t_n = t_{n+1} - t_n$ using implicit time stepping scheme as [16]:

$$\overrightarrow{\Delta\varepsilon_{vp}^n} = \Delta t_n \left((1-\Theta)\overrightarrow{\dot{\varepsilon}_{vp}^n} + \Theta\overrightarrow{\dot{\varepsilon}_{vp}^{n+1}}\right). \tag{15}$$

For $\Theta = 0$ the Euler time integration scheme is obtained which is also referred to as 'fully explicit' (or forward difference method) since the strain increment is completely determined from the existing conditions at time t_n. On the other hand, taking $\Theta = 1$ gives a 'fully implicit' (or backward difference) scheme with strain increment being determined from the strain rate corresponding to the end of the time interval. The case $\Theta = \frac{1}{2}$ results in the so-called 'implicit trapezodial' scheme which is also known generally as the Crank-Nicolson rule in the context of linear equation. To define $\dot{\varepsilon}_{vp}^{n+1}$ in Equation (15), the limited Taylor series expansion can be used [16]:

$$\overrightarrow{\dot{\varepsilon}_{vp}^{n+1}} = \overrightarrow{\dot{\varepsilon}_{vp}^n} + \overrightarrow{H^n} : \overrightarrow{\Delta\sigma^n}, \tag{16}$$

where,

$$\overrightarrow{H^n} = \overrightarrow{\frac{\partial \dot{\varepsilon}_{vp}^n}{\partial \sigma}} = H^n, \tag{17}$$

where $\Delta\sigma^n$ is the stress change occurring in the time interval $\Delta t_n = t_{n+1} - t_n$.
Thus Equation (15) can be written as:

$$\overrightarrow{\Delta\varepsilon_{vp}^n} = \overrightarrow{\dot{\varepsilon}_{vp}^n}\Delta t_n + \overrightarrow{C^n} : \overrightarrow{\Delta\sigma^n}, \tag{18}$$

where,

$$\overrightarrow{C^n} = \Theta\Delta t_n \overrightarrow{H^n}. \tag{19}$$

4. 2. Evaluation of Matrix H To use the fully implicit or semi-implicit (trapezoidal) time stepping scheme, the matrix C^n is required which in turn can be expressed in terms of H^n as indicated in Equation (17). Matrix H^n has to be explicitly determined for the yield surface assumed for material behavior. From Equations (12) and (17) we have:

$$\vec{\vec{H}} = \gamma\Phi\overrightarrow{\frac{\partial^2 F}{\partial \sigma^2}} + \gamma\frac{d\Phi}{dF}\left(\overrightarrow{\frac{\partial F}{\partial \sigma}} \otimes \overrightarrow{\frac{\partial F}{\partial \sigma}}\right), \tag{20}$$

where the symbol $\langle \quad \rangle$ on Φ and the superscript n are dropped for convenience. The only difficulty of computing $\vec{\vec{H}}$ for any criterion is deriving $\overrightarrow{\frac{\partial F}{\partial \sigma}}$ and especially $\overrightarrow{\frac{\partial^2 F}{\partial \sigma^2}}$ which is explained in detail in Section 3.

5. COMPUTATIONAL PROCEDURE

The essential steps in solving process can be summarized here. The solution begins from the known initial conditions at $t = 0$, which are the static elastic situation. At this stage d^0, F^0, ε^0 and σ^0 are known and $\varepsilon_{vp}^0 = 0$. The time marching scheme described in the previous section is then employed to advance the solution by one time stepping at a time. The solution sequence can be observed in Table 2.

TABLE 2. The solution sequence adopted in the current study.

Step 1 Suppose at time $t = t_n$ we have an equilibrium situation and $\vec{d}^n$, $\vec{\sigma}^n$, $\vec{\varepsilon}^n$, $\vec{\varepsilon}^n_{vp}$, $\vec{F}^n$ are known. The following quantities are calculated:

$$\vec{\vec{B}}^n = \vec{\vec{B}}_0 + \vec{\vec{B}}_{NL},$$

$$\overleftrightarrow{\vec{D}^n} = \left(\vec{\vec{D}}^{-1} + \vec{\vec{C}}^n\right)^{-1},$$

$$\vec{\vec{K}}^n_T = \int_\Omega \vec{\vec{B}}^{n\,T} : \overleftrightarrow{\vec{D}^n} : \vec{\vec{B}}^n d\Omega,$$

$$\overrightarrow{\dot{\varepsilon}^n_{vp}} = \gamma < \Phi > \frac{\overrightarrow{\partial F}^n}{\partial \sigma}.$$

Step 2 Compute the displacement increments $\overrightarrow{\Delta d}^n$:

$$\overrightarrow{\Delta d}^n = \vec{\vec{K}}^{n\,-1}_T : \overrightarrow{\Delta V}^n,$$

$$\overrightarrow{\Delta V}^n = \int_\Omega \vec{\vec{B}}^{n\,T} : \overleftrightarrow{\vec{D}^n} . \overrightarrow{\dot{\varepsilon}^n_{vp}} \Delta t_n d\Omega + \overrightarrow{\Delta f}^n.$$

Step 3 Calculate the stress increment $\overrightarrow{\Delta \sigma}^n$:

$$\overrightarrow{\Delta \sigma}^n = \overleftrightarrow{\vec{D}^n} : \left(\vec{\vec{B}}^n : \overrightarrow{\Delta d}^n - \overrightarrow{\dot{\varepsilon}^n_{vp}} \Delta t_n\right).$$

Step 4 Determine the total displacements and stresses:

$$\vec{d}^{n+1} = \vec{d}^n + \overrightarrow{\Delta d}^n,\ \vec{\sigma}^{n+1} = \vec{\sigma}^n + \overrightarrow{\Delta \sigma}^n.$$

Step 5 Calculate the viscoplastic strain rate:

$$\overrightarrow{\dot{\varepsilon}^{n+1}_{vp}} = \gamma < \Phi > \frac{\overrightarrow{\partial F}^{n+1}}{\partial \sigma}.$$

Step 6 Apply the equilibrium correction: First calculate $\vec{\vec{B}}^{n+1}$ using displacements $\vec{d}^{n+1}$ and substitute stresses $\vec{\sigma}^{n+1}$ into equilibrium forces $\vec{\Psi}^{n+1}$:

$$\vec{\Psi}^{n+1} = \int_\Omega \vec{\vec{B}}^{n+1\,T} \vec{\sigma}^{n+1} d\Omega + \vec{f}^{n+1},$$

add these to the vector of incremental pseudo loads for use in the next time step:

$$\overrightarrow{\Delta V}^{n+1} = \int_\Omega \vec{\vec{B}}^{n+1\,T} : \overleftrightarrow{\vec{D}^{n+1}} . \overrightarrow{\dot{\varepsilon}^{n+1}_{vp}} \Delta t_{n+1} d\Omega + \overrightarrow{\Delta f}^{n+1} + \overrightarrow{\Psi}^{n+1}.$$

Step 7 Check to see if the viscoplastic strain rate $\overrightarrow{\dot{\varepsilon}^{n+1}_{vp}}$ is small enough at each Gaussian integrating point throughout the structure (i.e. to within a specified tolerance), if so, steady state conditions are achieved and the solution is either terminated or the next load increment is applied. If $\overrightarrow{\dot{\varepsilon}^{n+1}_{vp}}$ is non-zero, return to Step 1 and repeat the entire procedure for the next time step.

6. RESULTS AND DISCUSIONS

In this part an internally pressurized elastic-viscoplastic thick walled cylinder as illustrated in Figure 3 is investigated. The mechanical properties are assumed as follows: Young modulus of elasticity ($E = 21000\ dN/mm^2$), Poisson' ratio ($\nu = 0.3$), yield stress ($F_0 = \sigma_Y = 24.0\ dN/mm^2$), plastic modulus ($H' = 0.0\ dN/mm^2$), fluidity parameter ($\gamma = 0.001/day$), inner radius of the cylinder ($a = 100\ mm$) and outer radius of the cylinder ($b = 200\ mm$), and the flow function $\Phi(F) = F$ .In order to verify the developed computer code, the explicit and implicit trapezoidal and the fully implicit time stepping schemes along with the von Mises criterion and associated flow rule are used. An explicit time stepping algorithm $(\Theta = 0)$ is initially employed and the variation of radial displacement at the inner surface with time can be observed in the curves of Figure 4. In the first one, the load increment $P = 14\ dN/mm^2$ is applied in one load step for two time steps$\tau = 0.01$ and 0.05. As it is seen, the reduction of accuracy is apparent with the larger time stepping which overestimating the viscoplastic strain rates. In the second one, the load increment $P = 14\ dN/mm^2$ is applied in two load steps, i.e. $12\ dN/mm^2$ and $2\ dN/mm^2$ for $\tau = 0.01$. As it is seen the convergence of two curves is acceptable (see Figure 4).

The initial time stepping was chosen as 0.1 days and the steady state convergence tolerance parameter was taken as 0.1 % as in Ref. [16]. The problem was then resolved, using the implicit trapezoidal time stepping scheme $(\Theta = 0.5)$ and the full implicit or backward difference scheme $(\Theta = 1)$. Good agreements between the three time integration schemes are evident in Figure 5.

Figure 6 shows the steady state hoop stress distributions for the time integration schemes $\Theta = 0$ and $\Theta = 1$. The results presented in Figures 4-6 are quite close to those of Ref. [16]. In the following, different investigations and comparisons are presented including comparison between the explicit, implicit trapezoidal and fully implicit time stepping schemes for both independent and dependent criteria to hydrostatic pressure. It is noted that in Ref. [16] only the solution for von Mises criteria was presented, however, with the current calculation approach, the second differentiation of a yield criterion the solution for any yield criterion can be achieved.

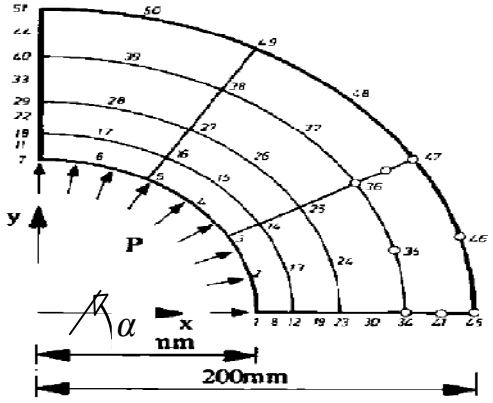

Figure 3. Mesh employed in the elastic-viscoplastic analysis of an internally pressurized thick cylinder under plane strain conditions.

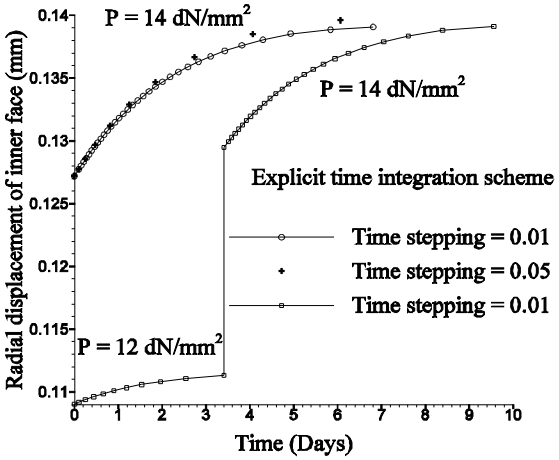

Figure 4. Variations of displacement with time at the inner surface for an elastic-viscoplastic cylinder subjected to an incrementally internal pressure.

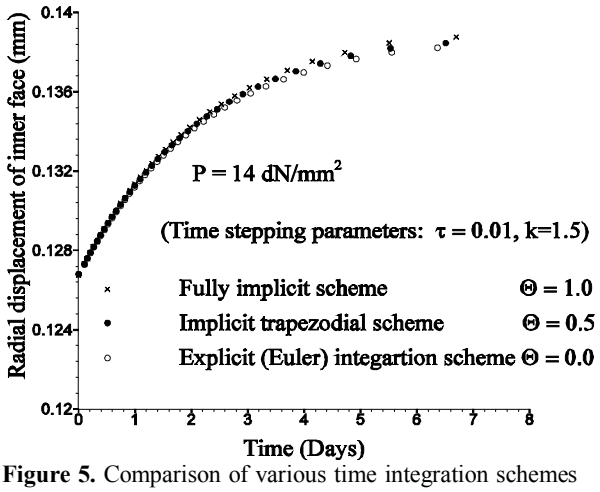

Figure 5. Comparison of various time integration schemes for internally pressurized cylinder.

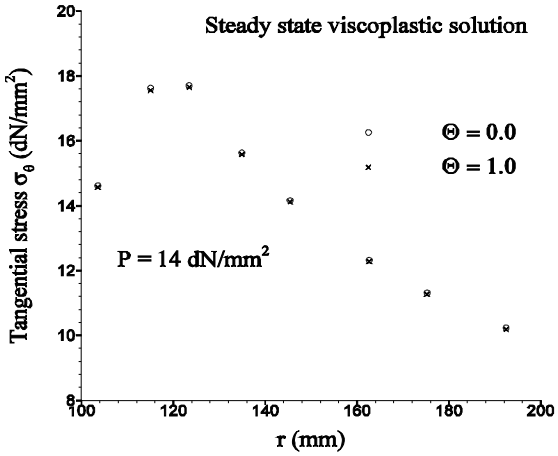

Figure 6. Distribution of steady state circumferential stress in an elastic-viscoplastic internally pressurized cylinder.

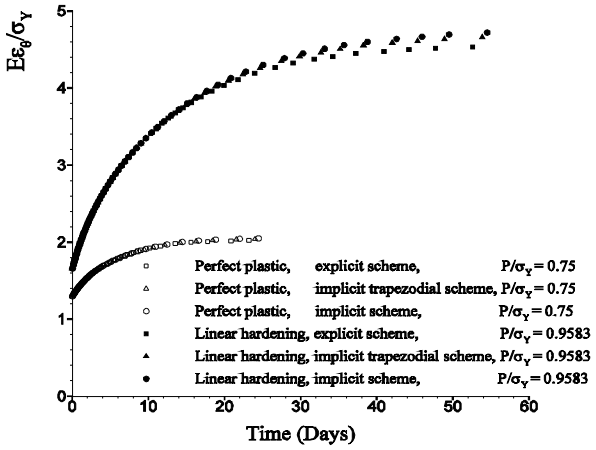

Figure 7. Variations of circumferential strain with time at the inner surface, using von Mises criterion.

In the following, different investigations and comparisons are presented including comparison between the explicit, implicit trapezoidal and fully implicit time stepping schemes for both independent and dependent criteria to hydrostatic pressure. It is noted that in Ref. [16] only the solution for von Mises criteria was presented, however, with the current approach of calculating the second differentiation of a yield criterion the solution for any yield criterion can be achieved. Figures 7-8 show the variation of circumferential strain of the inner surface $\left(\frac{r}{a}=1\right)$ with time and also the steady state circumferential stress distributions for $\left(1\le\frac{r}{a}\le 2\right)$ for explicit, implicit trapezoidal and fully implicit time stepping schemes while the von Mises criterion, perfect-plastic material

and linear isotropic hardening behavior, $H' = \frac{E}{10}$, are used and the geometry of the cylinder is assumed to be $\frac{b}{a} = 2$.

Figure 7 shows that with increasing time and development of plastic zone the differences between the results of three time stepping schemes increase. Moreover, the results of the trapezoidal implicit and fully implicit are more close to each other than those of explicit schemes. Furthermore, the circumferential strains predicted by the implicit time stepping scheme are larger than those predicted by the others. In addition, the steady hoop stresses predicted by the fully implicit time stepping scheme are smaller than those of the others, Figure 8.

The results show that the hardening increases the difference between three time stepping schemes. Figures 9-14 show the same parameters based on Tresca, Mohr-Coulomb and Drucker-Prager criteria, respectively. In using Mohr-Coulomb criterion, it is assumed that $tan\Phi = 0.879$. The linear isotropic hardening is assumed and the hardening module is taken as $H' = E/20$ and $H' = E/10\sqrt{3}$ for Mohr-Coulomb and Drucker-Prager criteria, respectively. The results show the same trend as explained for Figures 7 and 8, previously. Moreover, it is seen that the difference between the three time stepping schemes in Mohr-Coulomb and Drucker-Prager criteria are larger than those of Tresca and von-Mises criteria, respectively. In other words, when the yielding criteria are dependent on the hydrostatic pressure, the difference between the results obtained from the explicit, implicit trapezoidal and fully implicit time stepping schemes become more significant than those of the hydrostatic pressure independent yielding criterion. Furthermore, for non-linear isotropic hardening case this difference increases compared to perfect-plastic one.

The results obtained by the explicit, implicit trapezoidal and fully implicit time stepping schemes in steady state condition and experimental results are compared in Figure 15. This figure demonstrates the internal pressure in overstrain of 100% ($E\varepsilon_\theta/\sigma_Y = 1$) at external surface of the vessel with respect to the variation of ratio of external radius/internal radius, (b/a), for perfect-plastic material and von Mises criterion. The figure shows that using the fully implicit time stepping scheme could predict the experimental results more accurately. It is also observed that the difference between the numerical simulations and experimental data is maximum in $b/a = 1.6$ and is minimum in $b/a = 2.4$.

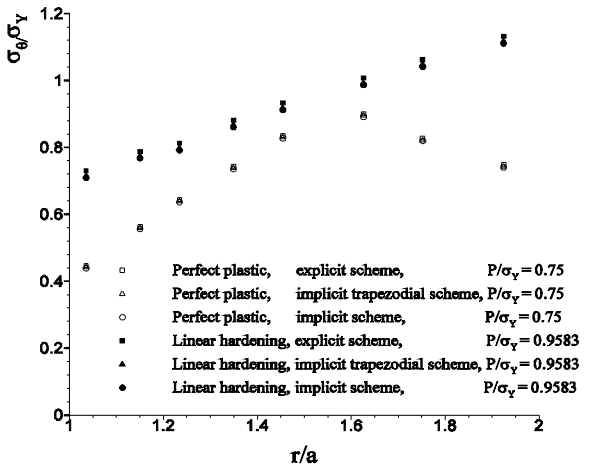

Figure 8. Distributions of steady state circumferential stress using von Mises criterion.

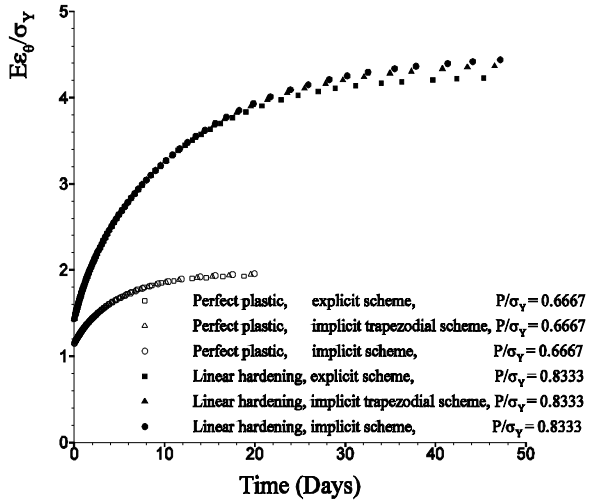

Figure 9. Variations of circumferential strain with time at the inner surface, using Tresca criterion.

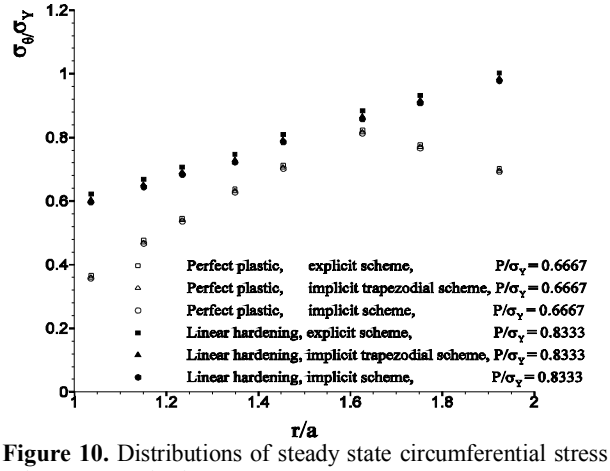

Figure 10. Distributions of steady state circumferential stress using Tresca criterion.

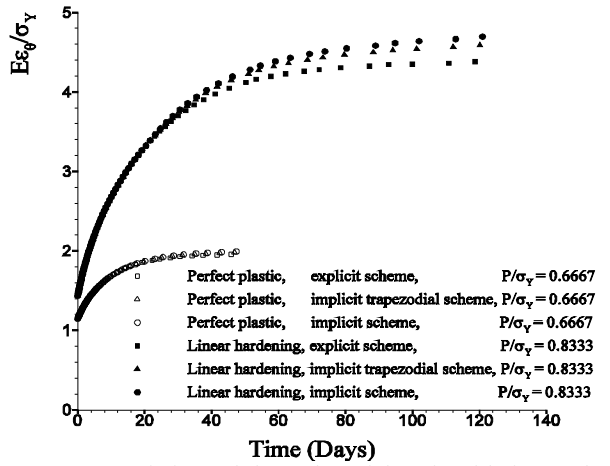

Figure 11. Variations of circumferential strain with time at the inner surface, using Mohr-Coulomb criterion.

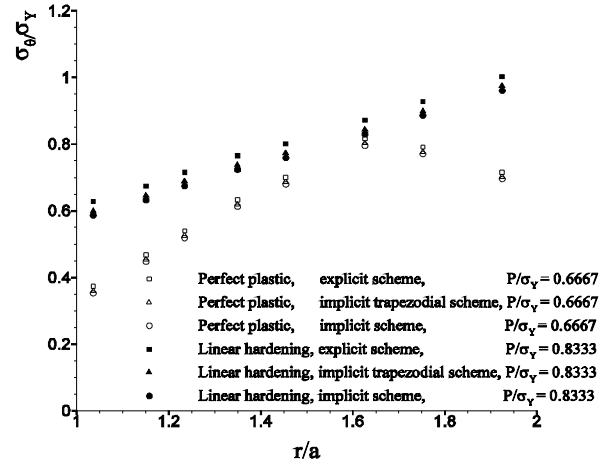

Figure 12. Distributions of steady state circumferential stress using Mohr-Coulomb criterion.

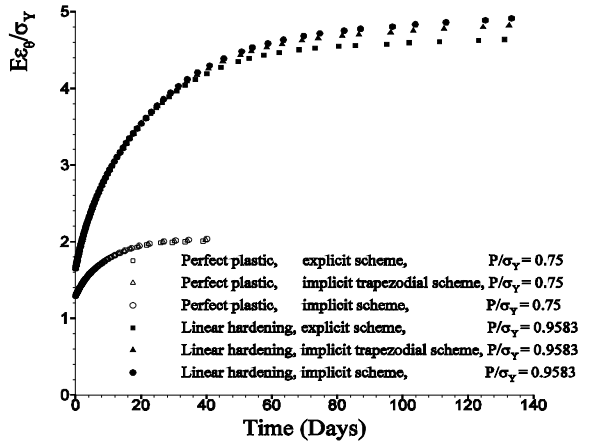

Figure 13. Variations of circumferential strain with time at the inner surface, using Drucker-Prager criterion.

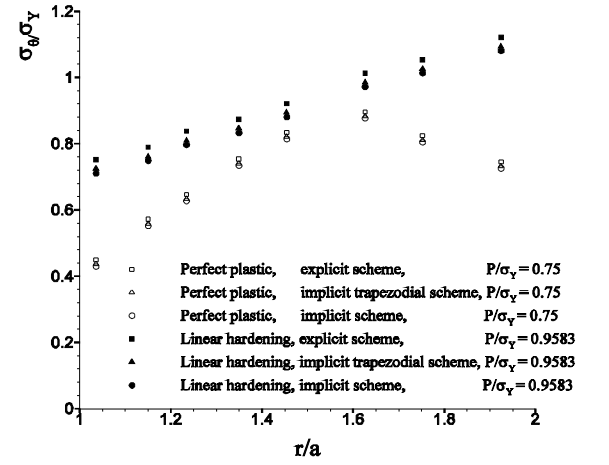

Figure 14. Distributions of steady state circumferential stress using Drucker-Prager criterion.

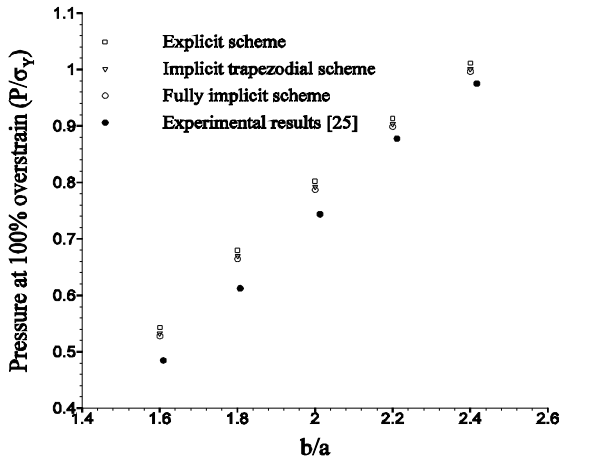

Figure 15. Comparison between the explicit, implicit trapezoidal and fully implicit time stepping schemes in steady state condition and experimental results.

7. CONCLUSIONS

The trapezoidal implicit and fully implicit time stepping schemes and also explicit time stepping schemes for different yield criteria along with the derivation of the second differentiation of the yield surface were studied. the results can be summarized as follows:

1- Applying more loads and development of plastic zone make the difference between the results more apparent.
2- The hydrostatic pressure dependent yield criteria were too sensitive in using time stepping schemes.
3- Implementing fully implicit time stepping scheme in rate-dependant plasticity predicts the experimental results more accurately than the other schemes.

8. REFERENCES

1. Krieg, R. and Krieg, D., "Accuracies of numerical solution methods for the elastic-perfectly plastic model", ***ASME, Transactions, Series J-Journal of Pressure Vessel Technology***, Vol. 99, (1977), 510-515.
2. Simo, J. C. and Taylor, R. L., "Consistent tangent operators for rate-independent elastoplasticity", ***Computer Methods in Applied Mechanics and Engineering***, Vol. 48, No. 1, (1985), 101-118.
3. Dodds Jr, R. H., "Numerical techniques for plasticity computations in finite element analysis", ***Computers & Structures***, Vol. 26, No. 5, (1987), 767-779.
4. Gratacos, P., Montmitonnet, P. and Chenot, J., "An integration scheme for prandtl-reuss elastoplastic constitutive equations", ***International Journal for Numerical Methods in Engineering***, Vol. 33, No. 5, (1992), 943-961.
5. Kadkhodayan, M. and Zhang, L., "A consistent dxdr method for elastic-plastic problems", ***International Journal for Numerical Methods in Engineering***, Vol. 38, No. 14, (1995), 2413-2431.
6. Kang, G., "A visco-plastic constitutive model for ratcheting of cyclically stable materials and its finite element implementation", ***Mechanics of Materials***, Vol. 36, No. 4, (2004), 299-312.
7. Nukala, P. K. V., "A return mapping algorithm for cyclic viscoplastic constitutive models", ***Computer Methods in Applied Mechanics and Engineering***, Vol. 195, No. 1, (2006), 148-178.
8. Ding, K., Qin, Q.-H. and Cardew-Hall, M., "Substepping algorithms with stress correction for the simulation of sheet metal forming process", ***International Journal of Mechanical Sciences***, Vol. 49, No. 11, (2007), 1289-1308.
9. Liang, L., Liu, Y. and Xu, B., "Design sensitivity analysis for parameters affecting geometry, elastic–viscoplastic material constant and boundary condition by consistent tangent operator-based boundary element method", ***International Journal of Solids and Structures***, Vol. 44, No. 7, (2007), 2571-2592.
10. Khosrou, S. A. and Sadrnezhad, S., "Substructure model for concrete behavior simulation under cyclic multiaxial loading", ***International Journal of Engineering***, (2008).
11. Romano, G., Barretta, R. and Diaco, M., "Algorithmic tangent stiffness in elastoplasticity and elastoviscoplasticity: A geometric insight", ***Mechanics Research Communications***, Vol. 37, No. 3, (2010), 289-292.
12. Rezaiee-Pajand, M. and S. Sinaie, "Nonlinear numerical integration scheme in strain space plasticity", ***International Journal of Engineering, Transactions A: Basics***, Vol. 24, (2011), 1-13.
13. Karrech, A., Seibi, A. and Duhamel, D., "Finite element modelling of rate-dependent ratcheting in granular materials", ***Computers and Geotechnics***, Vol. 38, No. 2, (2011), 105-112.
14. Voyiadjis, G. Z., Shojaei, A. and Li, G., "A generalized coupled viscoplastic–viscodamage–viscohealing theory for glassy polymers", ***International Journal of Plasticity***, Vol. 28, No. 1, (2012), 21-45.
15. Graham, S. M., Zhang, T., Gao, X. and Hayden, M., "Development of a combined tension–torsion experiment for calibration of ductile fracture models under conditions of low triaxiality", ***International Journal of Mechanical Sciences***, Vol. 54, No. 1, (2012), 172-181.
16. Owen, D. R. and Hinton, E., "Finite elements in plasticity", Pineridge Press Swansea, Vol. 271, (1980).
17. De Souza Neto, E. A., Peric, D. and Owen, D. R. J., "Computational methods for plasticity: Theory and applications", Wiley, (2011).
18. Simof, J. and Hughes, T., "Computational inelasticity", (2008).
19. Zienkiewicz, O. C. and Taylor, R. L., "The finite element method: Solid mechanics", Butterworth-heinemann, Vol. 2, (2000).
20. Crisfield, M. A., "Non-linear finite element analysis of solids and structures: Advanced topics", John Wiley & Sons, Inc., (1997).
21. Chakrabarty, J., "Theory of plasticity", Butterworth-Heinemann, (2006).
22. Chen, W.-F. and Zhang, H., "Structural plasticity: Theory, problems and cae software", Springer-Verlag New York, Inc., (1990).
23. Huang, S., "Continuum theory of plasticity", Wiley-Interscience, (1995).
24. Marcal, P., "A note on the elastic-plastic thick cylinder with internal pressure in the open and closed-end condition", ***International Journal of Mechanical Sciences***, Vol. 7, No. 12, (1965), 841-845.
25. Hill, R., "The mathematical theory of plasticity", Oxford: Clarendon Press, (1950)

APPENDIX I

The values of C_1, C_2 and C_3 are as following:

$$\begin{cases} C_1 = \frac{\partial F}{\partial J_1}, \\ C_2 = \frac{\partial F}{\partial J_2'} - \frac{tan\,3\theta}{2J_2'}\frac{\partial F}{\partial \theta}, \\ C_3 = \frac{-\sqrt{3}}{2\cos 3\theta}\frac{1}{(J_2')^{\frac{3}{2}}}\frac{\partial F}{\partial \theta}, \end{cases} \tag{A1.1}$$

These values are obtained for four famous criteria in Table A1.

The vectors $\overrightarrow{\frac{\partial J_1}{\partial \sigma}}$, $\overrightarrow{\frac{\partial J_2}{\partial \sigma}}$ and $\overrightarrow{\frac{\partial J_3}{\partial \sigma}}$ are independent from type of criterion and are as follows:

$$\overrightarrow{\frac{\partial J_1}{\partial \sigma}} = \begin{Bmatrix} 1 \\ 1 \\ 1 \\ 0 \\ 0 \\ 0 \end{Bmatrix},$$

$$\overrightarrow{\frac{\partial J_2}{\partial \sigma}} = \begin{Bmatrix} \sigma_x' \\ \sigma_y' \\ \sigma_z' \\ 2\tau_{yz} \\ 2\tau_{zx} \\ 2\tau_{xy} \end{Bmatrix}, \tag{A1.2}$$

$$\overrightarrow{\frac{\partial J_3}{\partial \sigma}} = \begin{Bmatrix} \sigma_y'\sigma_z' - \tau_{yz}^2 + \frac{J_2'}{3} \\ \sigma_x'\sigma_z' - \tau_{xz}^2 + \frac{J_2'}{3} \\ \sigma_x'\sigma_y' - \tau_{xy}^2 + \frac{J_2'}{3} \\ 2\left(\tau_{xz}\tau_{xy} - \sigma_x'\tau_{yz}\right) \\ 2\left(\tau_{xy}\tau_{yz} - \sigma_y'\tau_{xz}\right) \\ 2\left(\tau_{yz}\tau_{xz} - \sigma_z'\tau_{xy}\right) \end{Bmatrix}.$$

APPENDIX II

The vectors $\vec{C}_1^{'}, \vec{C}_2^{'}$ and $\vec{C}_3^{'}$ are as follows:

$$\vec{C}_1^{'} = \frac{\partial \vec{a}}{\partial J_1} = \{0 \quad 0 \quad 0 \quad 0 \quad 0 \quad 0\}^T,$$

$$\vec{C}_2^{'} = \frac{\partial \vec{a}}{\partial J_2^{'}} - \frac{tan\,3\theta}{2J_2^{'}}\frac{\partial \vec{a}}{\partial \theta} = \begin{Bmatrix} \sigma_x^{'} \\ \sigma_y^{'} \\ \sigma_z^{'} \\ 2\tau_{yz} \\ 2\tau_{zx} \\ 2\tau_{xy} \end{Bmatrix} + \left(\frac{\partial C_3}{\partial J_2^{'}} - \frac{tan\,3\theta}{2J_2^{'}}\frac{\partial C_3}{\partial \theta}\right)$$

$$\begin{Bmatrix} \sigma_y^{'}\sigma_z^{'} - \tau_{yz}^2 + \frac{J_2^{'}}{3} \\ \sigma_x^{'}\sigma_z^{'} - \tau_{xz}^2 + \frac{J_2^{'}}{3} \\ \sigma_x^{'}\sigma_y^{'} - \tau_{xy}^2 + \frac{J_2^{'}}{3} \\ 2\left(\tau_{xz}\tau_{xy} - \sigma_x^{'}\tau_{yz}\right) \\ 2\left(\tau_{xy}\tau_{yz} - \sigma_y^{'}\tau_{xz}\right) \\ 2\left(\tau_{yz}\tau_{xz} - \sigma_z^{'}\tau_{xy}\right) \end{Bmatrix} + C_3 \begin{Bmatrix} \frac{1}{3} \\ \frac{1}{3} \\ \frac{1}{3} \\ 0 \\ 0 \\ 0 \end{Bmatrix}, \tag{A2.1}$$

$$\vec{C}_3^{'} = \frac{-\sqrt{3}}{2\cos 3\theta}\frac{1}{(J_2^{'})^{\frac{3}{2}}}\frac{\partial \vec{a}}{\partial \theta} = \frac{-\sqrt{3}}{2\cos 3\theta}\frac{1}{(J_2^{'})^{\frac{3}{2}}}$$

$$\left(\frac{\partial C_2}{\partial \theta}\begin{Bmatrix} \sigma_x^{'} \\ \sigma_y^{'} \\ \sigma_z^{'} \\ 2\tau_{yz} \\ 2\tau_{zx} \\ 2\tau_{xy} \end{Bmatrix} + \frac{\partial C_3}{\partial \theta}\begin{Bmatrix} \sigma_y^{'}\sigma_z^{'} - \tau_{yz}^2 + \frac{J_2^{'}}{3} \\ \sigma_x^{'}\sigma_z^{'} - \tau_{xz}^2 + \frac{J_2^{'}}{3} \\ \sigma_x^{'}\sigma_y^{'} - \tau_{xy}^2 + \frac{J_2^{'}}{3} \\ 2\left(\tau_{xz}\tau_{xy} - \sigma_x^{'}\tau_{yz}\right) \\ 2\left(\tau_{xy}\tau_{yz} - \sigma_y^{'}\tau_{xz}\right) \\ 2\left(\tau_{yz}\tau_{xz} - \sigma_z^{'}\tau_{xy}\right) \end{Bmatrix}\right)$$

The matrices $\frac{\overleftrightarrow{\partial^2 J_1}}{\partial \sigma^2}$, $\frac{\overleftrightarrow{\partial^2 J_2^{'}}}{\partial \sigma^2}$ and $\frac{\overleftrightarrow{\partial^2 J_3^{'}}}{\partial \sigma^2}$ are as in (A 2.2):

$$\frac{\overleftrightarrow{\partial^2 J_1}}{\partial \sigma^2} = \begin{bmatrix} 0 & 0 & 0 & 0 & 0 & 0 \\ & 0 & 0 & 0 & 0 & 0 \\ & & 0 & 0 & 0 & 0 \\ & Sym. & & 0 & 0 & 0 \\ & & & & 0 & 0 \\ & & & & & 0 \end{bmatrix},$$

$$\frac{\overleftrightarrow{\partial^2 J_2^{'}}}{\partial \sigma^2} = \frac{1}{3}\begin{bmatrix} 2 & -1 & -1 & 0 & 0 & 0 \\ & 2 & -1 & 0 & 0 & 0 \\ & & 2 & 0 & 0 & 0 \\ & Sym. & & 6 & 0 & 0 \\ & & & & 6 & 0 \\ & & & & & 6 \end{bmatrix}, \tag{A2.2}$$

$$\frac{\overleftrightarrow{\partial^2 J_3^{'}}}{\partial \sigma^2} = \frac{2}{3}\begin{bmatrix} \sigma_x^{'} & \sigma_z^{'} & \sigma_y^{'} & -2\tau_{yz} & \tau_{xz} & \tau_{xy} \\ & \sigma_y^{'} & \sigma_x^{'} & \tau_{yz} & -2\tau_{xz} & \tau_{xy} \\ & & \sigma_z^{'} & \tau_{yz} & \tau_{xz} & -2\tau_{xy} \\ & Sym. & & -3\sigma_x^{'} & 3\tau_{xy} & 3\tau_{xz} \\ & & & & -3\sigma_y^{'} & 3\tau_{yz} \\ & & & & & -3\sigma_z^{'} \end{bmatrix}.$$

TABLE A 2.1. The values of $\frac{\partial C_i}{\partial J_2^{'}}$ for different yield criteria.

Yield criterion	$\frac{\partial C_1}{\partial J_2^{'}}$	$\frac{\partial C_2}{\partial J_2^{'}}$	$\frac{\partial C_3}{\partial J_2^{'}}$
Tresca	0	$-\frac{1}{2J_2^{'}}C_2$	$-\frac{1}{J_2^{'}}C_3$
von Mises	0	$-\frac{1}{2J_2^{'}}C_2$	0
Mohr-Coulomb	0	$-\frac{1}{2J_2^{'}}C_2$	$-\frac{1}{J_2^{'}}C_3$
Drucker-Prager	0	$-\frac{1}{2J_2^{'}}C_2$	0

APPENDIX III

Vectors $\vec{e}$, $\vec{f}$ and $\vec{g}$ along with the matrices $\overleftrightarrow{M}$ and $\overleftrightarrow{N}$ are presented in the (A 3.1):

$$\vec{e}^T = \left\{\sigma_x^{'} \quad \sigma_y^{'} \quad \sigma_z^{'} \quad 2\tau_{yz} \quad 2\tau_{zx} \quad 2\tau_{xy}\right\},$$

$$\vec{f} = \begin{Bmatrix} \sigma_y^{'}\sigma_z^{'} - \tau_{yz}^2 + \frac{J_2^{'}}{3} \\ \sigma_x^{'}\sigma_z^{'} - \tau_{xz}^2 + \frac{J_2^{'}}{3} \\ \sigma_x^{'}\sigma_y^{'} - \tau_{xy}^2 + \frac{J_2^{'}}{3} \\ 2\left(\tau_{xz}\tau_{xy} - \sigma_x^{'}\tau_{yz}\right) \\ 2\left(\tau_{xy}\tau_{yz} - \sigma_y^{'}\tau_{xz}\right) \\ 2\left(\tau_{yz}\tau_{xz} - \sigma_z^{'}\tau_{xy}\right) \end{Bmatrix},$$

$$\vec{g}^T = \left\{\frac{1}{3} \quad \frac{1}{3} \quad \frac{1}{3} \quad 0 \quad 0 \quad 0\right\},$$

$$\overleftrightarrow{M} = \begin{bmatrix} 2 & -1 & -1 & 0 & 0 & 0 \\ & 2 & -1 & 0 & 0 & 0 \\ & & 2 & 0 & 0 & 0 \\ & Sym. & & 6 & 0 & 0 \\ & & & & 6 & 0 \\ & & & & & 6 \end{bmatrix}, \tag{A3.1}$$

$$\overleftrightarrow{N} = \begin{bmatrix} \sigma_x^{'} & \sigma_z^{'} & \sigma_y^{'} & -2\tau_{yz} & \tau_{xz} & \tau_{xy} \\ & \sigma_y^{'} & \sigma_x^{'} & \tau_{yz} & -2\tau_{xz} & \tau_{xy} \\ & & \sigma_z^{'} & \tau_{yz} & \tau_{xz} & -2\tau_{xy} \\ & Sym. & & -3\sigma_x^{'} & 3\tau_{xy} & 3\tau_{xz} \\ & & & & -3\sigma_y^{'} & 3\tau_{yz} \\ & & & & & -3\sigma_z^{'} \end{bmatrix}$$

TABLE A 3.1. The values of C_i for the different yield criteria.

Yield criterion	C_1	C_2	C_3
Tresca	0	$\frac{\cos\theta}{(J_2^{'})^{\frac{1}{2}}}(1+\tan\theta\tan 3\theta)$	$\frac{\sqrt{3}}{J_2^{'}}\frac{\sin\theta}{\cos 3\theta}$
von Mises	0	$\frac{\sqrt{3}}{2(J_2^{'})^{\frac{1}{2}}}$	0
Mohr-Coulomb	$\frac{1}{3}\sin\Phi\frac{\cos\theta}{2(J_2^{'})^{\frac{1}{2}}}$	$[(1+tan\,\theta\,tan\,3\theta)+\frac{sin\,\Phi}{\sqrt{3}}$	$\frac{1}{2J_2^{'}cos\,3\theta}(\sqrt{3}\,sin\,\theta+cos\,\theta\,sin\,\Phi)$
Drucker-Prager	0	$\frac{1.0}{2(J_2^{'})^{\frac{1}{2}}}$	0

TABLE A 3.2. The values of $\frac{\partial C_i}{\partial\theta}$ for different yield criteria.

Yield criterion	$\frac{\partial C_1}{\partial\theta}$	$\frac{\partial C_2}{\partial\theta}$	$\frac{\partial C_3}{\partial\theta}$
Tresca	0	$-C_2\,tan\,\theta+\frac{1}{(J_2')^{\frac{1}{2}}}\left(\frac{tan\,3\theta}{cos\,\theta}+3\frac{sin\,\theta}{cos^2 3\theta}\right)$	$\frac{\sqrt{3}}{J_2'}\frac{1}{cos\,3\theta}(cos\,\theta+3\,sin\,\theta\,tan\,3\theta)$
von Mises	0	0	0
Mohr-Coulomb	0	$-C_2\,tan\,\theta+\frac{1}{2(J_2')^{\frac{1}{2}}}\left[\frac{tan\,3\theta}{cos\,\theta}+\frac{3\,sin\,\theta}{cos^2 3\theta}+\frac{sin\,\Phi}{\sqrt{3}}\left(\frac{3\,cos\,\theta}{cos^2 3\theta}-\frac{1}{cos\,\theta}\right)\right]$	$\frac{cos\,\theta}{2J_2'\,cos\,3\theta}[\sqrt{3}(1+3\,tan\,\theta\,tan\,3\theta)+sin\,\Phi\,(3\,tan\,3\theta-tan\,\theta)]$
Drucker-Prager	0	0	0

A General Solution for Implicit Time Stepping Scheme in Rate-dependant Plasticity

F. Moayyedian, M. Kadkhodayan

Department of Mechanical Engineering, Ferdowsi University of Mashhad, 91775-1111, Mashhad, Iran

P A P E R I N F O

Paper history:
Received 23 October 2012
Received in revised form 01 December 2012
Accepted 13 December 2012

Keywords:
Rate-dependant Plasticity
Time Stepping Schemes
Implicit
Thick Walled Cylinder

چکیده

در این پژوهش به دست آوردن مشتق مرتبه‌ی دوم یک سطح تسلیم با روش مرحله‌ای زمانی غیرصریح به همراه اپراتور الاستیک-پلاستیک سازگار با آن مورد مطالعه قرار گرفته است. در ادامه روش‌های مرحله‌ای زمانی صریح، ذورنقه‌ای غیرصریح و کاملاً غیرصریح در پلاستیسیته وابسته به زمان مقایسه شده‌اند. در پایان نشان داده شده است که استفاده از روش مرحله‌ای زمانی کاملاً غیرصریح در پلاستیسیته وابسته به زمان نتایج آزمایشگاهی را نسبت به دو روش دیگر دقیق‌تر پیش‌بینی میک‌ند.

doi: *10.5829/idosi.ije.2013.26.06c.09*